PNAS 108:373-378, 2011 **Classification: Biological Sciences; Neuroscience**

CAPS2 promotes BDNF secretion in hippocampal neurons and is critical for the development of hippocampal GABAergic interneuron networks

Yo Shinoda[1,2], Tetsushi Sadakata[1,2], Kazuhito Nakao[3], Ritsuko Katoh-Semba[1], Emi Kinameri[1], Asako Furuya[1], Yuchio Yanagawa[4], Hajime Hirase[3,5], Teiichi Furuichi[1,2,5,6*]

[1]Laboratory for Molecular Neurogenesis, RIKEN Brain Science Institute, Saitama 351-0198, Japan [2]JST-CREST, Saitama 332-0012, Japan [3]Hirase Research Unit, RIKEN Brain Science Institute, Saitama 351-0198, Japan [4]Gunma University Graduate School of Medicine, Gunma 371-8511, Japan [5]Saitama University Graduate School of Science and Engineering, Saitama 338-8570, Japan [6]Hiroshima University Graduate School of Biomedical Sciences, Hiroshima 734-8553, Japan

*Correspondence: Teiichi Furuichi Laboratory for Molecular Neurogenesis, RIKEN Brain Science Institute, 2-1 Hirosawa, Wako, Saitama 351-0198, Japan. Tel: +81-48-467-5906 Fax: +81-48-467-6079 E-mail: tfuruichi@brain.riken.jp

Abstract

Calcium-dependent protein for secretion 2 (CAPS2) is a dense-core vesicle associated protein that is involved in the secretion of brain-derived neurotrophic factor (BDNF). BDNF has a pivotal role in neuronal survival and development, including the development of inhibitory neurons and their circuits. However, it is largely unknown how CAPS2 affects BDNF secretion and what its biological significance in inhibitory neurons is. Here we reveal the role of CAPS2 in the regulated secretion of BDNF and show the effect of CAPS2 on the development of hippocampal GABAergic systems. We show that CAPS2 is colocalized with BDNF, both synaptically and extrasynaptically in axons of hippocampal neurons. Overexpression of exogenous CAPS2 in hippocampal neurons of CAPS2 knockout (KO) mice enhanced depolarization-induced BDNF exocytosis events in terms of kinetics, frequency and amplitude. We also show that in the CAPS2 KO hippocampus, BDNF secretion is reduced and GABAergic systems are impaired, including a decreased number of GABAergic neurons and their synapses, a decreased number of synaptic vesicles in inhibitory synapses and a reduced frequency and amplitude of mIPSCs. Conversely, excitatory neurons in the CAPS2 KO hippocampus were largely unaffected with respect to

fEPSPs, mEPSCs and synapse number and morphology. Moreover, CAPS2 KO mice exhibited several GABA system-associated deficits, including reduced late-phase long-term potentiation at CA3-CA1 synapses, decreased hippocampal theta oscillation frequency and increased anxiety-like behavior. Collectively, these results suggest that CAPS2 promotes activity-dependent BDNF secretion during the postnatal period, which is critical for the development of hippocampal GABAergic networks.

¥body

Introduction

Calcium-dependent activator protein for secretion (CAPS) was initially identified as a cytosolic protein associated with dense-core vesicles (DCVs) in endocrine and neuroendocrine cells and was implicated in Ca^{2+}-dependent DCV secretion (1-3). Neuronal CAPS is localized to DCVs where it is involved in Ca^{2+}-activated DCV exocytosis (2). A recent knockout (KO) mouse study suggested that CAPS proteins also play a role in priming glutamatergic synaptic vesicle (SV) exocytosis (4).

The CAPS protein family consists of two distinct members, CAPS1 and CAPS2 (5, 6). Our previous studies have shown that CAPS2 is involved in the secretion of brain-derived neurotrophic factor (BDNF) in cerebellar granule cells and cerebral cortical neurons (7, 8). BDNF plays a critical role in neuronal survival and differentiation and in synaptic development and plasticity (9-12). It also exhibits a neurotrophic action on the development of GABAergic interneurons and their networks in the cerebral cortex (13-15) and hippocampus (16, 17). BDNF is secreted from DCV-like secretory vesicles from neuronal dendrites and axons (18). Together with CAPS2, synaptotagmin-IV also controls BDNF secretion, although these two proteins act in opposite ways: CAPS2 promotes secretion (7, 8), whereas synaptotagmin-IV inhibits secretion (19). Little is known, however, about how CAPS2 affects the dynamics of BDNF secretion, while the biological significance of CAPS2-induced BDNF secretion is unknown.

In the present study we analyzed the role of CAPS2 in the regulation of BDNF secretion and in the development and function of hippocampal GABAergic neurons at cellular and microcircuitry levels. We discovered that expression of CAPS2 enhanced activity-dependent BDNF secretion kinetics, frequency and amplitude in hippocampal neurons from CAPS2 KO mice. Moreover, we found that CAPS2 KO mice have significant deficits in hippocampal GABAergic systems at multiple levels, ranging from inhibitory synaptic architectures and synaptic function, to related behaviors such as anxiety. Our results suggest an indispensable role of CAPS2 in enhancing BDNF

secretion, which is important for the proper development of hippocampal GABAergic interneuron networks.

Results Expression of exogenous CAPS2 enhances BDNF secretion in CAPS2 KO mouse hippocampal neurons

To investigate the function of CAPS2, we first examined its subcellular localization in cultured hippocampal neurons by immunocytochemistry (Fig. 1A). We found that CAPS2 immunopositive puncta were largely localized in tau-positive and MAP2-negative axons (supporting information Fig. S1). CAPS2 immunopositive puncta were colocalized with BDNF at 26.7% (Fig. 1A). However, only 17.7% of CAPS2 puncta that overlapped with BDNF were coincidently detected with bassoon puncta, indicating that the majority (82.3%) of CAPS2-associated BDNF vesicles was located at extrasynaptic sites rather than at presynaptic sites.

To monitor BDNF secretion from hippocampal neurons, we exogenously expressed BDNF-fused super-ecliptic pHluorin [a pH-sensitive green fluorescent protein (GFP) derivative] (20) whose fluorescence is quenched in the acidic lumen of vesicles, but which becomes fluorescent upon vesicle exocytosis due to the neutral pH outside of vesicles. In fixed wild-type neurons, fluorescent puncta of exogenous BDNF-pHluorin colocalized with endogenous CAPS2 immunosignals (Fig. 1B), as did endogenous BDNF immunosignals (Fig. 1A). To determine whether CAPS2 deficiency altered BDNF secretion, we performed time-lapse live-cell fluorescence imaging of BDNF-pHluorin in CAPS2 KO neurons with and without co-transfection of CAPS2-fused red fluorescent protein tdTomato (referred to as CAPS2+ and CAPS2cells, respectively) (Fig. 1C, D). Fluorescent puncta of BDNF-pHluorin and CAPS2-tdTomato colocalized in axons of co-transfected neurons (Fig. 1C), as did endogenous BDNF and CAPS2 immunosignals (Fig. 1A and Fig. S1). BDNF-pHluorin secretion was elicited by 50 mM KCl application in the presence of kynurenic acid and picrotoxin (inhibitors of excitatory and inhibitory transmission, respectively) (Fig. 1D and Video S1). Following co-transfection with CAPS2-tdTomato, the average number of BDNF-pHluorin puncta that appeared along neuronal axons during 8 min after KCl stimulation was significantly increased (CAPS2+: 95.4 ± 2.5 puncta/area *vs.* CAPS2-: 51.6 ± 8.3 puncta/area) (Fig. 1D, E). By contrast, the number of BDNF-pHluorin puncta before KCl stimulation (Fig. 1C), and the size of BDNF-pHluorin fluorescent puncta (Fig. S2) was not different between CAPS2+ and CAPS2- cells. BDNF-pHluorin secretion from CAPS2+ neurons was significantly faster than that from CAPS2- neurons (τ =217.9 s and 298.1 s, respectively) (Fig. 1F). Moreover, time-to-peak and peak frequency of BDNF-pHluorin secretion was significantly faster and larger, respectively, as a result of CAPS2-tdTomato co-transfection (time-to-peak in CAPS2+:

220 s *vs.* CAPS2-: 320 s; frequency in CAPS2+: 7.13 ± 1.22 *vs.* CAPS2-: 1.35 ± 0.38) (Fig. 1G).

Following KCl stimulation, analysis of single exocytosis events revealed more rapid appearance of fluorescent puncta in CAPS2+ neurons compared to CAPS2- neurons (Fig. 2). The fluorescence intensity of the majority of exocytosis events in CAPS2+ neurons was significantly greater compared to those in CAPS2- neurons (Fig. 2B). The average fractional change in fluorescence (ΔF/F) 8 min after KCl application was also larger in CAPS2+ neurons (161.6 ± 15.8) than in CAPS2- neurons (117.7 ± 2.8) (Fig. 2C). Taken together, these results suggest that CAPS2 promotes activity-dependent BDNF secretion in hippocampal neurons by enhancing the frequency, kinetics, and quantal size of BDNF vesicle exocytosis events.

Morphological abnormalities in GABAergic interneuron systems in the hippocampus of CAPS2 KO mice

The promotion of BDNF secretion by CAPS2 prompted the hypothesis that CAPS2 deficiency affects hippocampal neurons and synapses, for instance by affecting their development or maturation. To address this issue, we first compared hippocampal interneuronal development between WT and CAPS2 KO mice by counting glutamate decarboxylase (GAD) 67 promoter-driven GFP-tagged interneurons (see Supporting Information). We observed a reduction in the number of GFP-fluorescent interneurons in the CA1 and dentate gyrus of CAPS2 KO/GAD67-GFP mice compared to that in WT/GAD67-GFP mice during the adolescent (P28), but not adult, stage (Fig. S3). Next we compared hippocampal excitatory and inhibitory synapses between WT and CAPS2 KO mice by immunostaining with anti-vesicular glutamate transporter 1 (vGluT1, an excitatory presynapse marker) and anti-vesicular GABA transporter (vGAT, an inhibitory presynapse marker) (Fig. 3A, B). The number of vGluT1 immunopositive puncta in the CA1 stratum radiatum region was not different between WT and KO mice. Conversely, the number of vGAT immunopositive puncta was significantly decreased in CAPS2 KO mice at both P28 and 8 weeks (Fig. 3B): vGluT1 puncta at P28, WT = 68.6 ± 2.0 *vs*. KO 70.2 ± 2.4 and at 8 weeks, WT 66.4 ± 1.2 *vs*. KO 63.3 ± 1.7; vGAT puncta at P28, WT 35.9 ± 1.7 *vs*. KO 28.3 ± 1.9 and at 8 weeks, WT 33.5 ± 1.1 *vs*. KO 29.3 ± 1.2.

Moreover, electron microscopic analyses of inhibitory synaptic architectures in the CA1 region at 8 weeks revealed a decreased number and smaller distribution area of synaptic vesicles in CAPS2 KO mice compared to WT littermates (Fig. 3C-E). However, there was no significant difference in the number of excitatory synaptic vesicles or in their distribution between WT and CAPS2 KO mice (Fig. S4). These results suggest impaired development and/or survival of GABAergic interneurons during early postnatal stages in the CAPS2 KO mouse hippocampus,

which likely leads to or associates with deficits in inhibitory synapse architectures in adulthood.

Functional impairments in GABAergic interneuron systems in the hippocampus of CAPS2 KO mice, which likely affect GABAergic network activity and behavior

To determine whether developmentally impaired GABAergic interneurons affect inhibitory synaptic function in the CAPS2 KO hippocampus, miniature inhibitory postsynaptic currents (mIPSCs) were recorded in CA1 pyramidal cells of acute hippocampal slices (Fig. 4A-C). Juvenile CAPS2 KO mice (2-3 weeks old) exhibited significantly reduced mIPSC frequency compared with WT littermates (frequency per 3 min: number of peaks analyzed, WT = 8,350 [n=9] and CAPS2 KO = 11,146 [n=12]; amplitude: WT = 24.79 ± 2.26 pA and CAPS2 KO = 22.45 ± 1.79 pA; frequency: WT = 1.73 ± 0.11 Hz and CAPS2 KO = 1.06 ± 0.15 Hz) (Fig. 4B). In young adult CAPS2 KO mice (6-8 weeks old), significantly reduced mIPSC frequency and amplitude were observed (frequency per 3 min: number of peaks analyzed, WT = 15,843 [n=9] and CAPS2 KO = 10,000 [n=9]; amplitude: WT = 24.54 ± 2.43 pA and CAPS2 KO = 19.80 ± 1.41 pA; frequency: WT = 1.95 ± 0.25 Hz and CAPS2 KO = 0.69 ± 0.10 Hz) (Fig. 4C). In contrast, field excitatory postsynaptic potentials (fEPSPs) in the CA1 stratum radiatum were not significantly different in stimulus-response curves between CAPS2 KO and WT mice (Fig. S5A). In addition, the amplitude and frequency of miniature excitatory postsynaptic currents (mEPSCs) were unchanged in CAPS2 KOs (Fig. S5B), suggesting that excitatory neurons are not affected by CAPS2 KO.

We next examined whether the impaired synaptic transmission in inhibitory synapses of CAPS2 KOs affected synaptic plasticity at CA3-CA1 synapses. High-frequency stimulation-induced long-term potentiation (LTP) revealed no obvious differences between CAPS2 KO and WT mice (Fig. S5C). However, theta burst stimulation (TBS)-induced late-phase LTP (TBS-L-LTP) was impaired in CAPS2 KO mice (% baseline at 140 min: WT = 149.3 ± 5.2 %, CAPS2 KO = 133.0 ± 4.2 %) (Fig. 4D). BDNF is known to promote TBS-induced L-LTP at CA3-CA1 synapses (21); therefore, the reduced TBS-L-LTP might be due to reduced BDNF secretion in CAPS2 KO mice during TBS. However, bath application of recombinant BDNF did not completely ameliorate the reduced TBS-L-LTP in the CAPS2 KO mice (% baseline at 140 min: 141.6 ± 10.6 %) (Fig. S5D). On the other hand, picrotoxin, a GABAA receptor antagonist, abolished changes in TBS-L-LTP in CAPS2 KO mice (% baseline at 140 min: WT/PTX = 151.7 ± 6.0 %, CAPS2 KO/PTX = 160.8 ± 9.2 %) (Fig. 4E), suggesting a correlation between reduced TBS-L-LTP and impaired GABAergic neurotransmission in the CAPS2 KO mouse hippocampus.

Finally, we investigated the biological significance of enhanced BDNF secretion by CAPS2. In the hippocampus, GABAergic interneurons are involved in network activities, such as

hippocampal oscillation [for reviews, see (22)]. Notably, hippocampal electroencephalograms during the awake phase revealed significantly decreased theta oscillation frequency in the CA1 region of CAPS2 KO mice compared with WT littermates (Fig. S6). Impaired hippocampal GABA neurotransmission and decreased BDNF levels are thought to affect hippocampus-related learning and anxiety-like behavior (23-25). Interestingly, CAPS2 KO mice displayed increased anxiety-like behavior (Table S1), but showed little impairment in learning and memory tests. Together, these results suggest that reduced BDNF secretion in the CAPS2 KO hippocampus leads to significant deficits in the development and function of hippocampal GABAergic interneurons and synapses, thereby resulting in impaired hippocampal interneuronal network activity and behavior.

Discussion

The present study determined a regulatory role for CAPS2 in BDNF secretion kinetics and characterized the biological significance of CAPS2 in hippocampal GABAergic system development and function. These results revealed for the first time that CAPS2 enhances the kinetics, frequency and amplitude of regulated BDNF secretion from hippocampal neurons. In addition, the reduced BDNF secretion in CAPS2 KO mice resulted in impaired development and function of hippocampal GABAergic interneurons, synapses, networks and related behavior.

Time-lapse live-cell imaging of BDNF-pHluorin in the present study, demonstrated that CAPS2 protein positively controls BDNF release in terms of frequency, amplitude, and kinetics. CAPS2 KO neurons retained some degree of regulated BDNF secretion activity, despite decreased secretion and slow kinetics. Therefore, our results suggest that CAPS2 is critical for the enhancement of regulated BDNF secretion, but that CAPS2 is not essential for regulated secretion. Recent studies have shown that CAPS promotes *trans*-SNARE complex formation in DCV exocytosis (26), and an alternative pathway or proteins, such as Munc13-1 (27) and CAPS1 (4), could substitute for CAPS2 in CAPS2 KO neurons. In the latter study, CAPS2 was proposed to promote SV exocytosis. However, given our finding in hippocampal cell cultures that CAPS2 largely colocalizes with BDNF at bassoon-immunonegative extrasynaptic sites of axons, it is possible that the synaptic transmission defects observed in that study could be attributed to an indirect effect of CAPS2 on presynaptic function, such as SV recycling via regulation of BDNF release (28).

BDNF promotes GABAergic inhibitory interneuronal development (13-17). Previous results have demonstrated that knocked-down BDNF expression in cultured cortical neurons decreases the number of GABAergic synapses, resulting in reduced mIPSC frequency (29). Overexpression of the BDNF gene, as well as chronic treatment with BDNF, promotes maturation of GABAergic

innervations in the hippocampus (17). In the present study, several abnormalities were observed in hippocampal GABAergic interneurons of CAPS2 KO mice, in addition to the defective BDNF secretion kinetics. The number of vGAT-positive GABAergic synapses, number and distribution of SVs in inhibitory presynapses and mIPSC frequency and amplitude in the CA1 region were all reduced in CAPS2 KO mice. In contrast, CAPS2 KO mice did not exhibit changes in architecture or transmission properties of excitatory synapses compared with WT mice. Collectively, these results suggest a correlation between impaired BDNF secretion and defective GABAergic inhibitory neurons in the CAPS2 KO mouse hippocampus.

BDNF and GABA play a role in the modulation of synaptic plasticity. LTP enhancement and maintenance are associated with the activity-dependent BDNF signaling pathway (30). In addition, GABAergic neurotransmission influences LTP maintenance (31). The present study showed that TBS-L-LTP at CA3-CA1 synapses was significantly reduced in CAPS2 KO mice. Interestingly, acute BDNF application only partially rescued reduced TBS-L-LTP, while administration of the GABAA receptor antagonist, picrotoxin, completely abolished differences in TBS-L-LTP between CAPS2 KO and WT mice. Previous studies have demonstrated that the induction of LTP requires the inhibition of GABAergic transmission by GABAB autoreceptor activation (32) and/or GABAB receptor mediated GABAA receptor disinhibition (33). In the hippocampus of CAPS2 KO mice, impaired development and physiology of GABAergic neurons, which are not acutely ameliorated by BDNF, might compromise these GABAergic actions required for TBS-L-LTP.

GABAergic interneuronal activity is thought to influence neuronal network activities, such as theta oscillations (34), which are critical for temporal coding of neuronal ensembles and modification of synaptic efficacy (22). Moreover, theta oscillation (35) and the hippocampal GABAergic system play a prominent role in certain forms of emotional processing, with special emphasis on anxiety-like behavior (23-25). The present study showed that CAPS2 KO mice exhibited not only decreased frequency of hippocampal theta oscillations but also increased anxiety-like behavior. Thus, we suggest that CAPS2-mediated secretion may contribute to GABA- or BDNF-related network activities and may play a role in psychiatric behavior.

In conclusion, the present study demonstrated for the first time that CAPS2 promotes regulated BDNF secretion by affecting BDNF release kinetics. Our results also showed that enhanced BDNF secretion by CAPS2 is indispensable for proper development and function of hippocampal GABAergic neurons and synapses. This suggests that the loss of enhanced BDNF secretion by a deficit of CAPS2 causes impairments in hippocampal GABAergic interneuronal networks, resulting in impaired CA3-CA1 L-LTP and hippocampal theta oscillations and increased

anxiety-like behavior. Further studies are needed to elucidate the detailed mechanisms of CAPS2-mediated promotion of BDNF secretion kinetics and to gain a deeper understanding of the biological function of CAPS2.

Materials and methods

Detailed experimental procedures are described in the Supplemental Information.

Animals

All experimental protocols were approved by the RIKEN Institutional Animal Care and Use Committee.

Hippocampal primary cell culture and transfection

Primary hippocampal neurons from CAPS2 KO mice were prepared and cultured according to a previously described method (36), with slight modifications. Briefly, on days 6-8 *in vitro*, neurons were transfected with BDNF-4xpHluorin, with or without CAPS2-tdTomato, using lipofectamine 2000 (Invitrogen, San Diego, CA, USA). Twenty-four to 48 h after transfection, time-lapse live-cell imaging was performed.

Time-lapse imaging of BDNF secretion

For time-lapse experiments, glass-bottom culture dishes were transferred to a warm chamber (Tokai Hit, Shizuoka, Japan), and bathing saline solution (119 mM NaCl, 2.5 mM KCl, 2 mM $CaCl_2$, 2 mM $MgCl_2$, 30 mM glucose, 25 mM HEPES, 1 mM kynurenic acid, and 100 μM picrotoxin) was perfused into the recording chamber at room temperature via a thermo controller (Warner Instruments, Hamden, CT, USA), and then removed via a circulation controller (K.T. Labs, Saitama, Japan). Images of BDNF-pHluorin and CAPS2-tdTomato expression were sequentially acquired at 5 sec intervals using a Nikon ECLIPSE TE2000-E inverted microscope with a CoolSNAP HQ2-cooled CCD camera (Photometrics, Tucson, AZ, USA). Images were acquired by MetaMorph software. The number of fluorescent puncta in each area (24 μm × 24 μm) was quantified every 5 sec, and the values were plotted as a cumulative curve over a period of 10 min.

Hippocampal slice preparation and electrophysiology

Acute hippocampal slice preparations were prepared according to previously described methods (37), with slight modifications. mIPSCs were recorded in the presence of 1 mM kynurenic acid (TCI, Tokyo, Japan) and 1 μM tetrodotoxin (Tocris, Bristol, UK). mEPSCs were recorded in the presence

of 100 μm picrotoxin and 1 μM tetrodotoxin.

Immunocytochemistry and immunohistochemistry

Immunochemical staining of hippocampal cultures and slices was performed as previously described (7). The following antibodies were utilized: guinea pig polyclonal anti-CAPS2 (8) (1:10,000), rabbit polyclonal anti-BDNF (38) (1:200), mouse monoclonal anti-Bassoon (Stressgen, Ann Arbor, MI, USA) (1:500), guinea pig anti-vGluT1 (Millipore, Billerica, MA, USA) (1:2000) and mouse monoclonal anti-vGAT (Synaptic Systems, Goettingen, Germany) (1:500). The number of interneuron terminals in CA1 stratum radiatum regions of interest (10 μm × 10 μm) was quantified.

Electron microscopy

Electron microscopy was performed using a previously described method (39), with slight modifications. Under deep Nembutal anesthesia, wild-type and CAPS2 KO mice were transcardially perfused with 4% paraformaldehyde/2% glutaraldehyde/0.1 M phosphate buffer (pH 7.4). Serial ultrathin sections (70 nm thick) were stained with uranyl acetate/lead citrate. Interneuron terminals were distinguished by previously reported criteria (40).

Acknowledgments

We thank R.Y. Tsien for kindly providing tdTomato and J.E. Rothman for pHluorin. This study was supported by research grants from Ministry of Education, Culture, Sports, Science and Technology, Japan Science and Technology Agency and Japan Society for the Promotion of Science.

Figure Legends

Figure 1. CAPS2 enhances BDNF secretion in hippocampal neurons (A, B) Colocalization of CAPS2 and bassoon with (A) endogenous BDNF or (B) exogenously expressed BDNF-pHluorin in wild-type hippocampal cultures. Colocalization of BDNF (or BDNF-pHluorin) and CAPS2 in synapses (arrows) and in extrasynaptic zones (filled arrowheads), and CAPS2 without BDNF (or BDNF-pHluorin) in synapses (open arrowheads) are indicated. Scale bar, 10 μm. (C) Hippocampal neurons from CAPS2 KO mice were transfected with BDNF-pHluorin, with (top row) or without (bottom row) CAPS2-tdTomato. Scale bar, 2 μm. (D) BDNF-pHluorin exocytosis events were induced by 50 mM KCl stimulation during 0-8 min (thick bar at bottom). Images at every 2 min between 2 min before and 8 min after stimulation are shown. Scale bar, 2 μm. (E) Number of total events during an 8 min recording. Error bars represent SEM. *P<0.05 using Student's t-test. (F) Cumulative distribution of BDNF-pHluorin fluorescence events in the presence (red) and absence (black) of CAPS2-tdTomato. The thick bar indicates the duration of 50 mM KCl stimulation. *P<0.05 using the Kolmogorov-Smirnov test. (G) Histogram of events in the presence (red) and absence (gray) of CAPS2-tdTomato (E-G: n=12 cells from 3 [CAPS2+] and 4 [CAPS2–] different cultures per transfection).

Figure 2. Dynamics of BDNF-pHluorin secretion events (A) Representative time-lapse images of depolarization-induced single BDNF-pHluorin exocytosis events in axons of CAPS2 KO hippocampal neurons co-transfected with (top: CAPS2+) and without (bottom: CAPS2–) CAPS2-tdTomato. Images are shown in each 1 min between 2 min before and 8 min after the onset of 50 mM KCl stimulation at 0 min (third panel on the left). Scale bar, 1 μm. (B) Sample traces of BDNF-pHluorin fluorescence dynamics induced during 50 mM KCl stimulation (bar at bottom). Inset: horizontal bar 100 sec; vertical bar, 100 ΔF/F. (C) Average traces of BDNF-pHluorin fluorescence dynamics in the presence and absence of CAPS2-tdTomato. 50 mM KCl stimulation is indicated by thick bar. Average traces were normalized to maximum punctum fluorescence intensity prior to depolarization. Between 160 and 480 sec after 50mM KCl administration, CAPS2+ mice (n = 28 from 3 different cultures) exhibited an average intensity of 169.5 ± 18.3, whereas CAPS2- mice (n = 36 from 4 different cultures) exhibited an average intensity of 105.2 ± 2.4 (P<0.01, Student's t-test). Error bars indicate ± SEM.

Figure 3. Morphological abnormalities of GABAergic interneurons in the CAPS2 KO mouse hippocampus (A) Representative immunofluorescence images of vGluT1 and vGAT in the hippocampal CA1 region of WT and CAPS2 KO mice at P28 and 8 weeks. St. pyr, stratum pyramidale; St. rad, stratum radiatum. Scale bar, 10 μm. (B) Number of vGluT1- and vGAT-positive

puncta in the stratum radiatum. Error bars represent SEM. *P<0.05, using Student's t-test (n=12, 16, 14, and 14 regions in P28 WT and CAPS2 KO mice, and 8-week-old WT and CAPS2 KO mice, respectively, from at least 6 slices from 3 mice for each). (C) Representative ultrastructure of GABAergic terminals. Scale bar, 250 nm. (D-E) Number of SVs per GABAergic terminal (D) and area of SV distribution (E). Error bars represent SEM. **P<0.01 and ***P<0.001 using Student's t-test (n=26, 29 synapses in 8-week-old WT and CAPS2 KO mice, respectively, from 6 pictures from 3 mice for each genotype).

Figure 4. Functional impairments of GABAergic interneurons in the CAPS2 KO mouse hippocampus (A) Examples of mIPSCs in 8-week-old WT and CAPS2 KO mice. Scales: horizontal bar, 100 ms; vertical bar, 100 pA. (B-C) Cumulative plot of mIPSC frequency (left), mean amplitude (middle) and frequency (right) in 2- to 3-week-old (B) and 6- to 8-week-old (C) WT and CAPS2 KO mice. *P<0.05 using the Kolmogorov-Smirnov test for cumulative plot. *P<0.05, **P<0.01 and ***P<0.001 using Student's t-test for mean amplitude and frequency. Error bars represent SEM. (at 2-3 week old: n=9 from 4 WT mice, n=12 from 5 CAPS2 KO mice; at 6-8 week old: n=9 from 4 WT mice, n=9 from 5 CAPS2 KO mice). (D) Time course of TBS-induced LTP at CA3-CA1 synapses (left). Results 120 min after TBS (right) (n=10 each for WT and CAPS2 KO mice from 5 and 7 mice of each genotype). Error bars represent SEM. *P<0.05 using Student's t-test. Inset: representative traces immediately before (left) and 120 min after (right) TBS for each genotype. Horizontal bar, 10 ms; vertical bar, 1 mV. (E) Time course of TBS-LTP in the presence of picrotoxin (left). Results 120 min after TBS (right) (n=9, 9 slices for 6- to 8-week-old WT and CAPS2 KO mice from 4 and 5 mice for each genotype). Error bars represent SEM. Inset: representative traces immediately before (left) and 120 min after (right) TBS for each genotype. Horizontal bar, 10 ms; vertical bar, 200 μV.

References

1. Walent JH, Porter BW, & Martin TF (1992) A novel 145 kd brain cytosolic protein reconstitutes Ca(2+)-regulated secretion in permeable neuroendocrine cells. Cell 70:765-775.
2. Berwin B, Floor E, & Martin TF (1998) CAPS (mammalian UNC-31) protein localizes to membranes involved in dense-core vesicle exocytosis. Neuron 21:137-145.
3. Tandon A, et al. (1998) Differential regulation of exocytosis by calcium and CAPS in semi-intact synaptosomes. Neuron 21:147-154.
4. Jockusch WJ, et al. (2007) CAPS-1 and CAPS-2 are essential synaptic vesicle priming proteins. Cell 131:796-808.
5. Cisternas FA, Vincent JB, Scherer SW, & Ray PN (2003) Cloning and characterization of human CADPS and CADPS2, new members of the Ca2+-dependent activator for secretion protein family. Genomics 81(3):279-291.
6. Speidel D, et al. (2003) A family of Ca2+-dependent activator proteins for secretion: comparative analysis of structure, expression, localization, and function. J Biol Chem 278(52):52802-52809.
7. Sadakata T, et al. (2007) Autistic-like phenotypes in Cadps2-knockout mice and aberrant CADPS2 splicing in autistic patients. J Clin Invest 117:931-943.
8. Sadakata T, et al. (2004) The secretory granule-associated protein CAPS2 regulates neurotrophin release and cell survival. J Neurosci 24:43-52.
9. Greenberg ME, Xu B, Lu B, & Hempstead BL (2009) New insights in the biology of BDNF synthesis and release: implications in CNS function. J Neurosci 29:12764-12767.
10. Huang EJ & Reichardt LF (2001) Neurotrophins: roles in neuronal development and function. Annu Rev Neurosci 24:677-736.
11. Lu B, Pang PT, & Woo NH (2005) The yin and yang of neurotrophin action. Nat Rev Neurosci 6:603-614.
12. McAllister AK, Katz LC, & Lo DC (1999) Neurotrophins and synaptic plasticity. Annu Rev Neurosci 22:295-318.
13. Rutherford LC, DeWan A, Lauer HM, & Turrigiano GG (1997) Brain-derived neurotrophic factor mediates the activity-dependent regulation of inhibition in neocortical cultures. J Neurosci 17(12):4527-4535.
14. Kohara K, et al. (2003) Inhibitory but not excitatory cortical neurons require presynaptic brain-derived neurotrophic factor for dendritic development, as revealed by chimera cell culture. J Neurosci 23(14):6123-6131.
15. Hong EJ, McCord AE, & Greenberg ME (2008) A biological function for the neuronal activity-dependent component of Bdnf transcription in the development of cortical inhibition. Neuron 60(4):610-624.
16. Marty S, et al. (1996) Brain-derived neurotrophic factor promotes the differentiation of various hippocampal nonpyramidal neurons, including Cajal-Retzius cells, in organotypic slice cultures. J Neurosci 16:675-687.
17. Yamada MK, et al. (2002) Brain-derived neurotrophic factor promotes the maturation of GABAergic mechanisms in cultured hippocampal neurons. J Neurosci 22:7580-7585.
18. Matsuda N, et al. (2009) Differential activity-dependent secretion of brain-derived

neurotrophic factor from axon and dendrite. J Neurosci 29(45):14185-14198.
19. Dean C, et al. (2009) Synaptotagmin-IV modulates synaptic function and long-term potentiation by regulating BDNF release. Nat Neurosci 12(6):767-776.
20. Miesenbock G, De Angelis DA, & Rothman JE (1998) Visualizing secretion and synaptic transmission with pH-sensitive green fluorescent proteins. Nature 394(6689):192-195.
21. Schinder AF & Poo M (2000) The neurotrophin hypothesis for synaptic plasticity. Trends Neurosci 23:639-645.
22. Buzsáki G (2002) Theta oscillations in the hippocampus. Neuron 33:325-340.
23. Zheng F, et al. (2009) Activin tunes GABAergic neurotransmission and modulates anxiety-like behavior. Mol Psychiatry 14(3):332-346.
24. Papadopoulos T, et al. (2007) Impaired GABAergic transmission and altered hippocampal synaptic plasticity in collybistin-deficient mice. EMBO J 26(17):3888-3899.
25. Earnheart JC, et al. (2007) GABAergic control of adult hippocampal neurogenesis in relation to behavior indicative of trait anxiety and depression states. J Neurosci 27:3845-3854.
26. James DJ, Kowalchyk J, Daily N, Petrie M, & Martin TF (2009) CAPS drives trans-SNARE complex formation and membrane fusion through syntaxin interactions. Proc Natl Acad Sci U S A 106(41):17308-17313.
27. Garcia-Junco-Clemente P, Linares-Clemente P, & Fernandez-Chacon R (2005) Active zones for presynaptic plasticity in the brain. Mol Psychiatry 10(2):185-200.
28. Lessmann V (1998) Neurotrophin-dependent modulation of glutamatergic synaptic transmission in the mammalian CNS. Gen Pharmacol 31(5):667-674.
29. Bramham CR & Messaoudi E (2005) BDNF function in adult synaptic plasticity: the synaptic consolidation hypothesis. Prog Neurobiol 76:99-125.
30. Meredith RM, Floyer-Lea AM, & Paulsen O (2003) Maturation of long-term potentiation induction rules in rodent hippocampus: role of GABAergic inhibition. J Neurosci 23:11142-11146.
31. Davies CH, Starkey SJ, Pozza MF, & Collingridge GL (1991) GABA autoreceptors regulate the induction of LTP. Nature 349:609-611.
32. Mott DD & Lewis DV (1991) Facilitation of the induction of long-term potentiation by GABAB receptors. Science 252(5013):1718-1720.
33. Paulsen O & Moser EI (1998) A model of hippocampal memory encoding and retrieval: GABAergic control of synaptic plasticity. Trends Neurosci 21:273-278.
34. Siok CJ, Taylor CP, & Hajos M (2009) Anxiolytic profile of pregabalin on elicited hippocampal theta oscillation. Neuropharmacology 56(2):379-385.
35. Shiraishi Y, Mizutani A, Yuasa S, Mikoshiba K, & Furuichi T (2004) Differential expression of Homer family proteins in the developing mouse brain. J Comp Neurol 473:582-599.
36. Liu L, et al. (2004) Role of NMDA receptor subtypes in governing the direction of hippocampal synaptic plasticity. Science 304(5673):1021-1024.
37. Katoh-Semba R, Takeuchi IK, Semba R, & Kato K (1997) Distribution of brain-derived neurotrophic factor in rats and its changes with development in the brain. J Neurochem 69(1):34-42.
38. Sadakata T, et al. (2007) Impaired cerebellar development and function in mice lacking CAPS2, a protein involved in neurotrophin release. J Neurosci 27(10):2472-2482.

39. Harris KM & Landis DM (1986) Membrane structure at synaptic junctions in area CA1 of the rat hippocampus. Neuroscience 19(3):857-872.

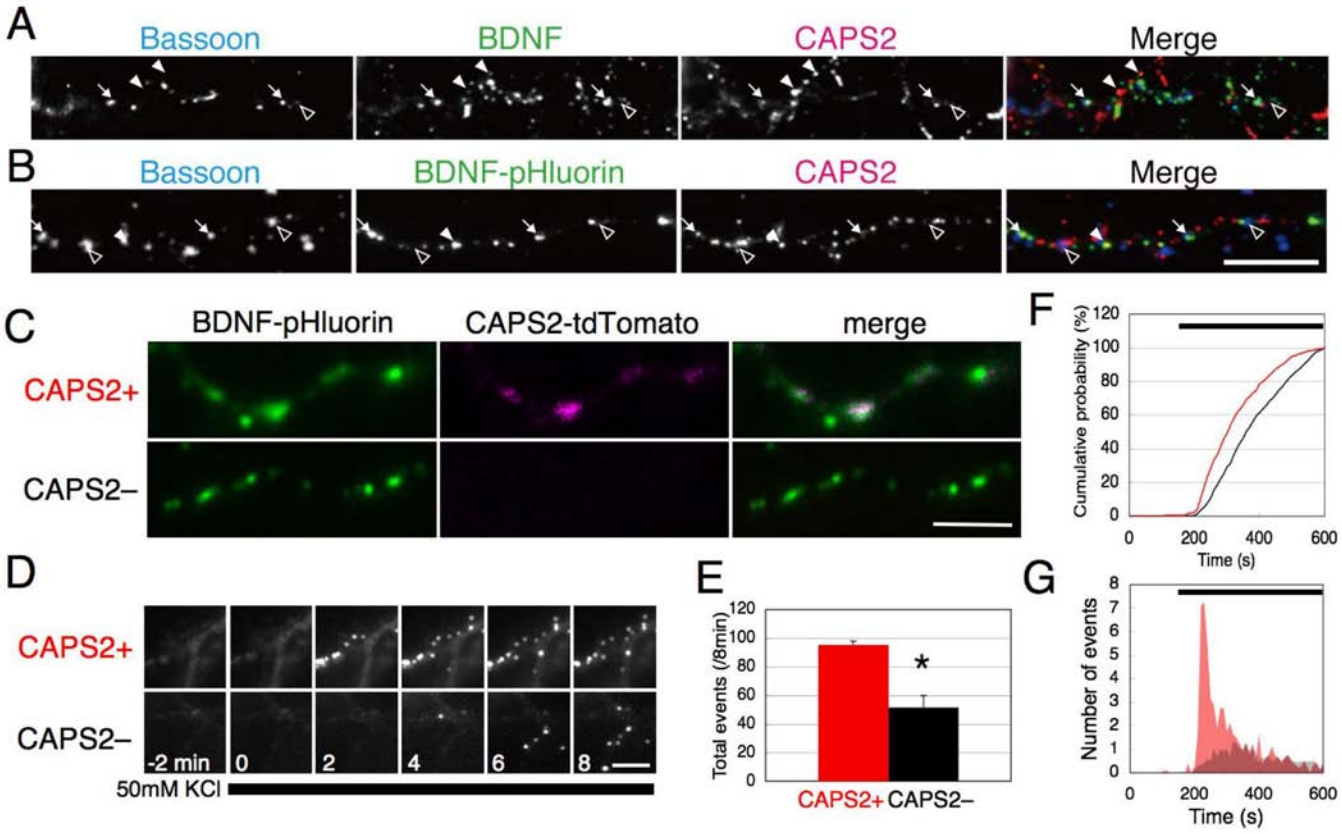
A
Bassoon
BDNF
CAPS2
Merge
B
Bassoon
BDNF-pHluorin
CAPS2
Merge
C
BDNF-pHluorin
CAPS2-tdTomato
merge
CAPS2+
CAPS2–
D
CAPS2+
CAPS2–
-2 min
0
2
4
6
8
50mM KCl
E
Total events (/8min)
120
100
80
60
40
20
0
*
CAPS2+
CAPS2–
F
Cumulative probability (%)
120
100
80
60
40
20
0
0
200
400
600
Time (s)
G
Number of events
8
7
6
5
4
3
2
1
0
0
200
400
600
Time (s)

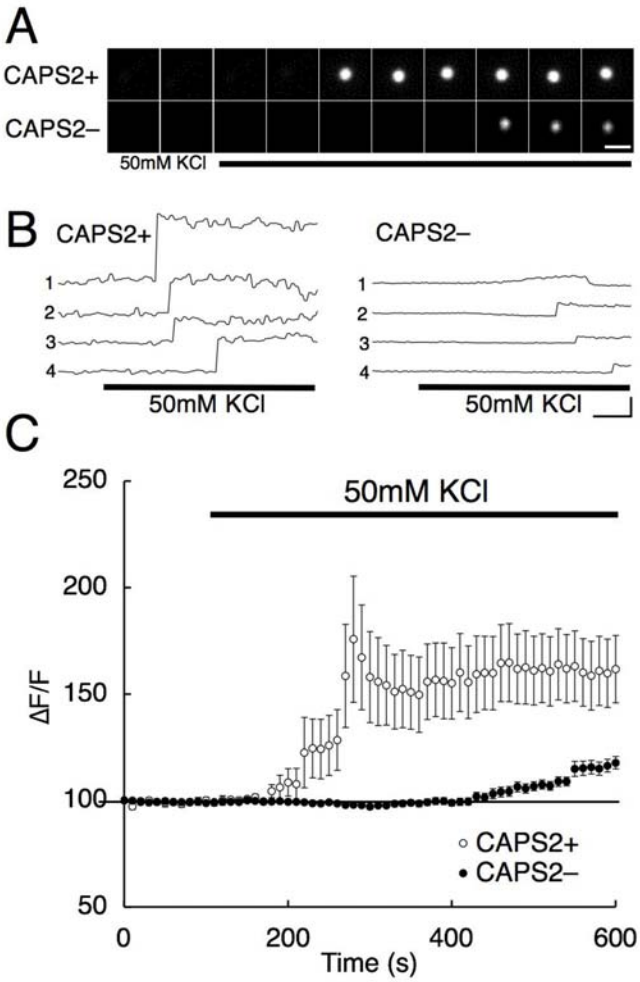
A
CAPS2+
CAPS2–
50mM KCl
B
CAPS2+
CAPS2–
1
2
3
4
50mM KCl
50mM KCl
C
50mM KCl
250
200
150
100
50
ΔF/F
CAPS2+
CAPS2–
0
200
400
600
Time (s)

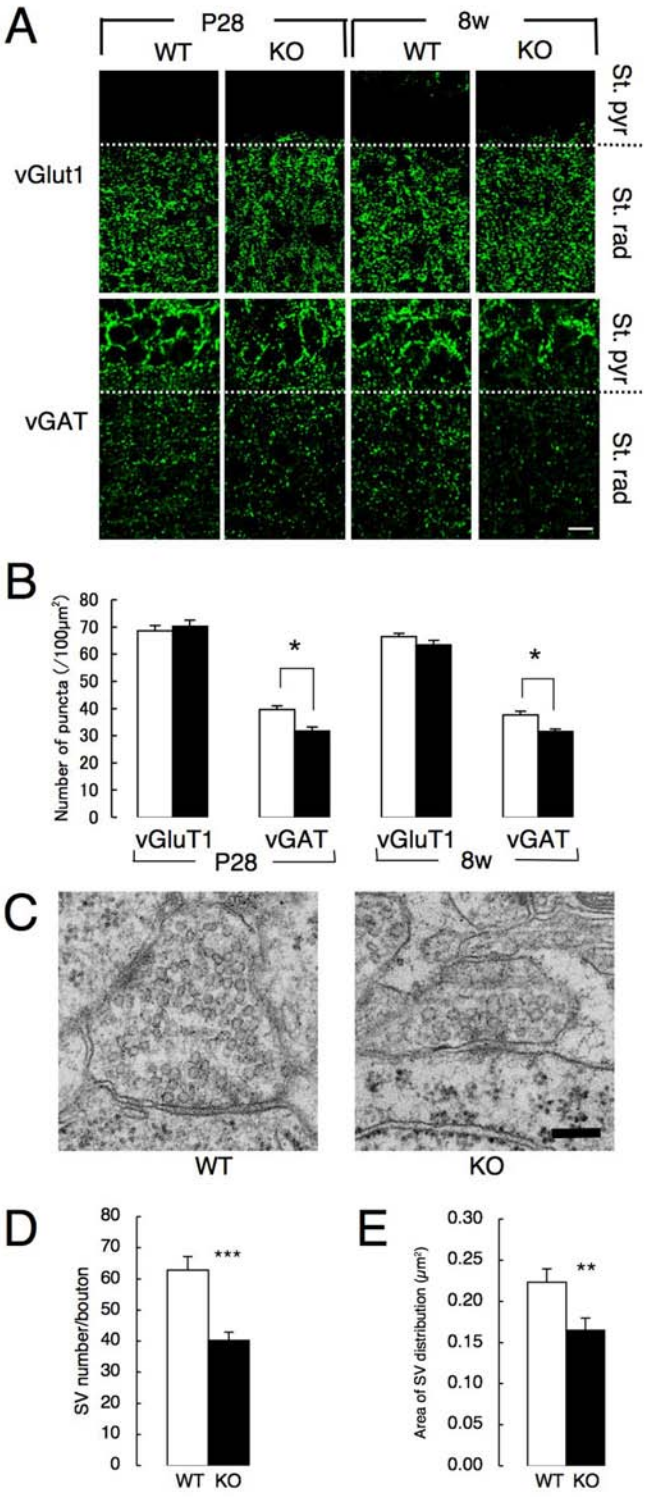
A
P28
8w
WT
KO
WT
KO
St. pyr
St. rad
vGlut1
St. pyr
St. rad
vGAT
B
Number of puncta (/100μm²)
80
70
60
50
40
30
20
10
0
*
*
vGluT1
vGAT
vGluT1
vGAT
P28
8w
C
WT
KO
D
SV number/bouton
80
70
60
50
40
30
20
10
0
***
WT KO
E
Area of SV distribution (μm²)
0.30
0.25
0.20
0.15
0.10
0.05
0.00
**
WT KO

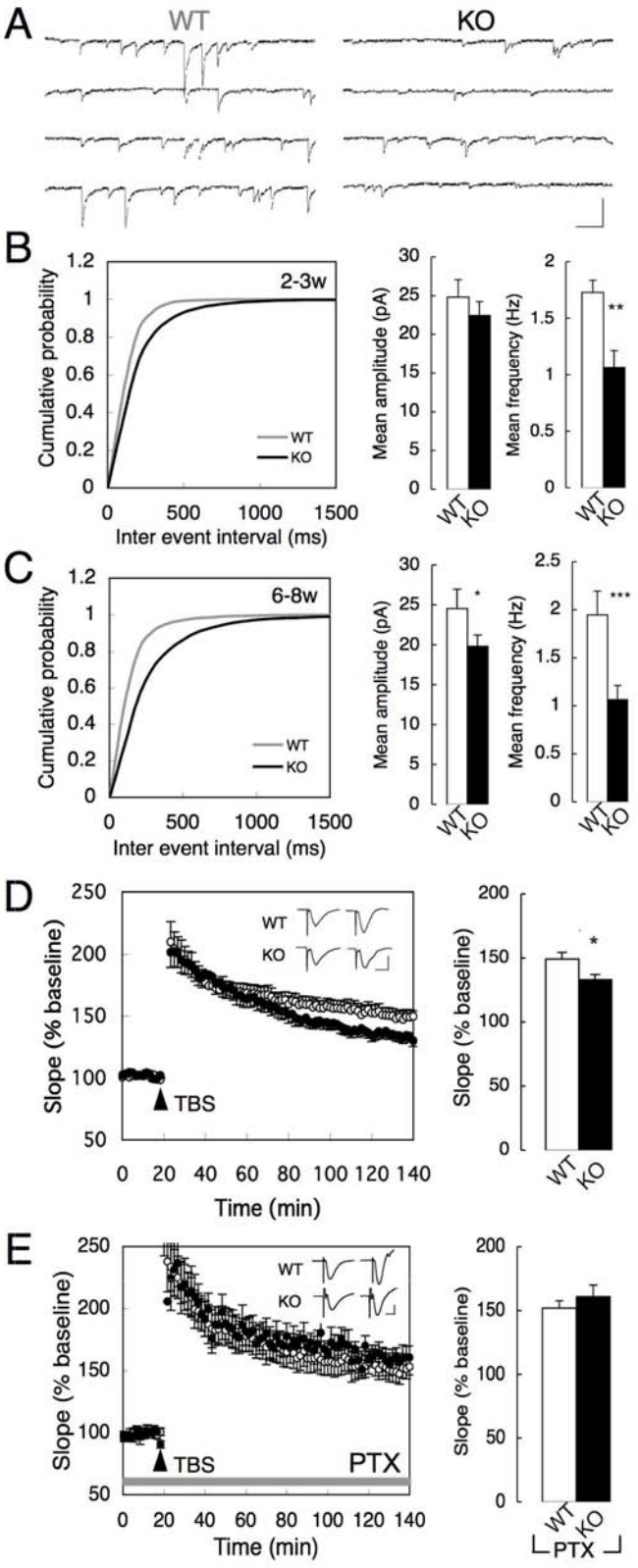
A
WT
KO
B
2-3w
Cumulative probability
Inter event interval (ms)
WT
KO
Mean amplitude (pA)
Mean frequency (Hz)
**
C
6-8w
Cumulative probability
Inter event interval (ms)
WT
KO
Mean amplitude (pA)
Mean frequency (Hz)
*
***
D
Slope (% baseline)
WT
KO
TBS
Time (min)
Slope (% baseline)
*
E
Slope (% baseline)
WT
KO
TBS
PTX
Time (min)
Slope (% baseline)
PTX

Supporting Information

CAPS2 promotes BDNF secretion in hippocampal neurons and is critical for the development of hippocampal GABAergic interneuron networks

Yo Shinoda, Tetsushi Sadakata, Kazuhito Nakao, Ritsuko Katoh-Semba, Emi Kinameri, Asako Furuya, Yuchio Yanagawa, Hajime Hirase, and Teiichi Furuichi

1. Author Contributions

YS, TS, and TF directed the project. YS conducted all imaging, histology, *in vitro* electrophysiology, electron microscopy and behavioral experiments. KN and HH performed and analyzed the *in vivo* electron encephalogram experiment. RKS conducted the enzyme immunoassay experiments. EK and AF produced cell cultures and constructed the plasmids. YY provided the GAD67-GFP knock-in mice. YS wrote the original draft of the manuscript, which was amended by TF.

2. Figure Legends

Figure S1. CAPS2 immunopositive puncta are localized in axons but not in dendrites in cultured hippocampal neurons. CAPS2 immunopositive puncta are localized in Tau immunopositive axons (upper) but not in MAP2 immunopositive dendrites (lower). Scale bar, 10 μm.

Figure S2. CAPS2 over-expression does not increase the size of BDNF-pHluorin fluorescent puncta. Quantitation of the average size of BDNF-pHluorin fluorescent puncta in CAPS2-tdTomato over-expressing (CAPS2+) and CAPS2 knockout (CAPS2-) neurons (n=57, 63 in WT and KO mice, respectively). Error bars represent SEM.

Figure S3. GABAergic interneuron numbers are reduced at P28, but recover by 8 weeks, in the CAPS2 KO mouse hippocampus. (A) Representative pictures of P28 and 8-week-old WT and CAPS2 KO mouse hippocampi. GABAergic interneurons were visualized by crossing CAPS2 KO mice with GAD67-GFP knock-in mice. The dentate gyrus (DG), CA3 and CA1 regions were analyzed. Scale bar, 100 μm. (B) Number of GFP-positive interneurons in WT and CAPS2 KO mice. The number of GFP neurons is

reduced in the CA1 and DG of CAPS2 KO mice at P28, but there is no difference between WT and KO at 8 weeks of age (n=9, 9 and n=6, 6 in P28 and 8-week-old WT and KO mice, respectively). Error bars represent SEM. *P<0.05 and ***P<0.001 using Student's t-test.

Figure S4. Number and distribution of SVs per excitatory terminal is indistinguishable between WT and CAPS2 KO mice. Number of SVs per excitatory terminal (A) and area of SV distribution (B). Error bars represent SEM (n=146, 175 in 8-week-old WT and CAPS2 KO mice, respectively).

Figure S5. Basal transmission and HFS-induced CA3-CA1 LTP are unchanged in the CAPS2 KO mouse hippocampus but TBS-induced LTP and the effect of BDNF are impaired. (A) I/O curve in the hippocampus remains unchanged between WT and KO mice. Representative fEPSP traces of WT and CAPS2 KO mice are shown at the top of the panel. Scales: horizontal bar, 10 ms; vertical bar, 2 mV. Average fEPSP slope vs. amplitude of fiber volley (bottom) (n=13 slices for WT and n=14 slices for KO from 4 and 5 mice of each genotype, respectively). (B) Representative traces of mEPSCs recorded from neurons in the hippocampal CA1 region in WT and CAPS2 KO slices (upper). Statistical data of mEPSC amplitude (bottom left) and frequency (bottom right) are shown. mEPSC amplitude and frequency are unchanged in CAPS2 KO mice (n=9 cells/slices each for WT and KO from 3 mice of each genotype). Error bars represent SEM. Scales: horizontal bar, 100 ms; vertical bar, 10 pA (C) Time course of CA3-CA1 LTP induced by HFS (left). Results 120 min after HFS (right) (n=13 slices for WT and n=14 slices for KO from 5 and 6 mice of each genotype, respectively). Error bars represent SEM. Inset shows representative traces immediately before (left) and 120 min after (right) HFS in each genotype. Inset: horizontal bar, 10 ms; vertical bar, 1 mV. (D) Time course of TBS-LTP with 100 ng/ml BDNF application (grey bar) indicated (Fig. 4D) (left). Results 120 min after TBS (right) (for BDNF experiment, n=10 CAPS2 KO slices from 5 mice, WT and CAPS2 KO data are replicated from Fig. 4D). Error bars represent SEM. *P<0.05 using one-way ANOVA and post-hoc Dunnett's t-test (n=10 slices in each group). Inset shows representative traces immediately before (left) and 120 min after (right) TBS in each genotype. Scales: horizontal bar, 10 ms; vertical bar, 1 mV.

Figure S6. Reduction of the frequency of hippocampal CA1 theta oscillations in

awake CAPS2 KO mice. Theta oscillations were recorded from the hippocampal CA1 region from unanesthetized mice during REM sleep (upper traces) and from awake mobile mice (lower traces). Note that the peak frequency of theta oscillations is shifted to the left in the KO (black) compared with the WT (gray), as indicated by arrows in the logarithmic frequency scale plots (left plots).

Video S1. Time-lapse live-cell imaging of BDNF-pHluorin secretion from CAPS2 KO mouse hippocampal neurons transfected with CAPS2-tdTomato, related to Figures 1 and 2. This video is an example of pHluorin fluorescence dynamics on a axon 2 min before and 8 min after 50 mM KCl stimulation. KCl stimulation was applied at 2 min, as shown in the video.

3. Experimental Procedures

Generation of CAPS2 KO mice carrying the GAD67-EGFP transgene and analysis of GABAergic interneurons

The generation of CAPS2 KO mice was previously described (1). CAPS2 KO ($CAPS2^{-/-}$) and WT littermates containing the GAD67 promoter-driven GFP transgene were generated by breeding CAPS2 heterozygous ($CAPS2^{+/-}$) mice with GAD67-GFP knock-in heterozygous ($GAD67^{GFP/+}$) mice (2). Genotyping was performed by PCR. $CAPS2^{+/+}GAD67^{GFP/+}$ (WT/GAD67-GFP) and $CAPS2^{-/-}GAD67^{GFP/+}$ (KO/GAD67-GFP) mice were generated by crossing $CAPS2^{+/-}GAD67^{GFP/+}$ mice with $CAPS2^{+/-}$ mice. The numbers of GFP-fluorescent interneurons in the CA1, CA3 and DG regions of interest (200 mm × 200 mm) were quantified.

DNA expression constructs

The BDNF cDNA (3) was fused to four tandem repeated sequences of super ecliptic pHluorin (generously provided by Dr. J.E. Rothman, Sloan-Kettering Institute, USA), and was subcloned into pEF-BOS to create pEF-BOS-BDNF-4xpHluorin. The CAPS2 cDNA (3) was fused to tdTomato (Clontech) and subcloned into pEF-BOS to create pEF-BOS-CAPS2-tdTomato.

Hippocampal primary cell cultures and transfection

Primary cultured hippocampal neurons from CAPS2 KO mice were prepared using previously described methods (4), with slight modifications. Briefly, CAPS2 KO mouse

hippocampi were dissected on P0, dissociated, and plated onto poly-D-lysine-coated glass bottom dishes (MatTek, US). On days 6–8 *in vitro*, neurons were transfected with BDNF-4xpHluorin, with or without CAPS2-tdTomato, using Lipofectamine 2000 (Invitrogen). Twenty-four to 48 h after transfection, time-lapse live-cell imaging was performed. Transfected cells, which emitted green (BDNF-4xpHluorin) fluorescence and/or red (CAPS2-tdTomato) fluorescence, were used for subsequent imaging experiments.

Hippocampal slice preparation and electrophysiology

Acute hippocampal slice preparations were prepared according to previously described methods (5), with slight modifications. Briefly, under deep anesthesia, CAPS2 WT and KO mice (2 to 3 weeks old and 6 to 8 weeks old) were decapitated and the brains were rapidly removed. Transverse hippocampal slices (400-500 μm in thickness) were cut using a vibratome (PRO 7, Dosaka, Japan) and were maintained in artificial cerebrospinal fluid (ACSF) at room temperature. A bipolar platinum iridium-stimulating electrode was placed in the CA1 stratum radiatum region. Field excitatory postsynaptic potentials (fEPSPs) were recorded from the CA1 stratum radiatum following a 0.05-Hz test pulse. LTP was electrically induced using one of the following protocols. High frequency stimulation (HFS)-induced long-term potentiation (LTP) was elicited by 100Hz, 100pulses stimulation. Theta-burst stimulation (TBS)-induced LTP was elicited by four trains, with 10-s intervals between trains. Each train had five bursts separated by 200 ms and included four pulses delivered at 100 Hz, which were at 20% of maximal stimulus intensity. For LTP recording during the inhibition of GABAergic transmission, 100 μM picrotoxin (Sigma, USA) was dissolved in ACSF. For LTP recording in the presence of BDNF, recombinant BDNF (100 ng/ml) and BSA (1 μg/ml) were applied during the LTP experiment at least 20 min prior to TBS. Whole-cell patch-clamp recordings were performed from CA1 pyramidal neurons under visual guidance using IR-DIC optics (Hamamatsu Photonics, Japan). Patch pipettes (2-5 MΩ) were pulled from borosilicate glass capillaries (GC150F-10, Harvard Apparatus, UK). Data were amplified using a MultiClamp 700A (Molecular Devices, USA) and were digitized at 10 kHz and filtered at 2 kHz using a Digidata 1440 system with pCLAMP9 software (Molecular Devices, USA). Cells with a high-seal resistance >1 GΩ and a series resistance <25 MΩ, were included in the analysis. Series- and input-resistance were controlled before and after each recording and cells were discarded if one or both

parameters were altered by >20%. Miniature inhibitory postsynaptic currents (mIPSCs) were pharmacologically isolated using bath application of 1 mM kynurenic acid (TCI, Japan) and 1 μM tetrodotoxin (Tocris). Miniature excitatory postsynaptic currents (mEPSCs) were pharmacologically isolated using bath application of 100 μM picrotoxin (SIGMA, USA) and 1μM tetrodotoxin (Tocris). Cells were voltage clamped to -80 mV, and mIPSCs and mEPSCs were recorded for 3 min. The high-sucrose cutting solution contained (mM): 234 sucrose, 2.5 KCl, 1.25 NaH_2PO_4, 0.5 $CaCl_2$, 10 $MgSO_4$, 26 $NaHCO_3$ and 11 D-glucose, gassed with 95% O_2/5% CO_2. ACSF contained (mM): 125 NaCl, 2.5 KCl, 1.25 NaH_2PO_4, 2 $CaCl_2$, 1 $MgCl_2$, 26 $NaHCO_3$ and 11 D-glucose, gassed with 95% O_2/5% CO_2. The intracellular solution contained (mM): 124 CsCl, 8 KCl, 8 NaCl, 10 HEPES, 0.1 EGTA, 4 MgATP, 0.3 NaGTP and 5 QX-314 (Sigma) for mIPSC recording. CsCl was replaced with cesium methanesulfonate for mEPSC recording.

Immunohistochemistry and immunocytochemistry

Immunochemical staining of hippocampal cultures and slices was performed as described previously (1). For immunohistochemistry, P28 and 8-week-old C57BL/6J mice were anesthetized with diethyl ether and were transcardially perfused with saline, followed by 4% paraformaldehyde/PBS. Brains were dissected, post-fixed in 4% paraformaldehyde at 4°C for 5 h, and cryoprotected by immersion in 15% sucrose/PBS overnight at 4°C. After embedding in Tissue-Tek OCT compound (Sakura Finetechnical), brains were frozen in dry ice powder and 14 μm sagittal sections were cut using a cryostat (Leica CM1850; Leica Microsystems) at -18°C. Sections were then air-dried for 1 h and rinsed three times in PBS. For immunocytochemistry, cultured neurons were fixed with 4% paraformaldehyde/PBS and then washed with PBS. After blocking with 5% normal donkey serum/PBS (Vector Laboratories), sections were incubated with primary antibody at 4°C overnight, rinsed in PBS, incubated with secondary antibody at room temperature for 1 h and then rinsed in PBS. Sections were then mounted with Vectashield Mounting Medium (Vector Laboratories) and examined using an epifluorescent microscope (Eclipse E800; Nikon) equipped with a cooled charge-coupled device camera (SPOT model 1.3.0; Diagnostic Instruments) or with a confocal laser microscope (FV1000; Olympus). Antibodies used were as follows: guinea pig polyclonal anti-CAPS2 antibody (Sadakata et al., 2004) (1:10000), rabbit polyclonal anti-BDNF antibody (Katoh-Semba et al., 1997)

(1:100), mouse monoclonal anti-Tau antibody (BD Biosciences) (1:1000), mouse monoclonal anti-MAP2 antibody (Sigma) (1:500), guinea pig polyclonal anti-vGluT1 antibody (Chemicon) (1:2000), and mouse monoclonal anti-vGAT antibody (Synaptic systems) (1:500). The number of excitatory and inhibitory terminals in the CA1 stratum radiatum region of interest (10 μm × 10 μm) was quantified.

Electron microscopy

Under deep Nembutal anesthesia (250 mg/Kg, i.p.), 3-month-old WT and CAPS2 KO mice were transcardially perfused with 2 ml saline followed by 20 ml 4% paraformaldehyde/2% glutaraldehyde/0.1 M phosphate buffer (pH 7.4). The brains were removed and immersed in the same fixative at 4°C overnight. Transverse hippocampal slices (300 μm thick) were cut using a microtome (VT1000S, Leica) and were post-fixed in cold 1% OsO_4 solution for 1 hr at 4°C. Following dehydration in a series of graded alcohols, the sections were embedded in epoxy resin (EPON812, Taab, UK). Serial ultrathin sections (70 nm thick) were cut using an ultramicrotome, mounted on 200 μm mesh, uncoated, copper grids, and then stained with uranyl acetate/lead citrate. Dendritic profiles were serially traced and examined using an electron microscope (JEM-1200EX, Jeol, Japan), and digital image data from imaging plates were scanned and digitized using the FDL imaging system (Fujifilm, Tokyo, Japan). Digitized images were processed using Image Gauge (Fujifilm, Tokyo, Japan) and Photoshop (Adobe).

Behavioral experiments

Open field test

Open field tests, with or without a novelty object, were performed as previously described (1) using 3-month-old male mice. Locomotor activity was measured in an open field apparatus (60 × 60 cm), with 50 lux at the surface level. Each mouse was placed in the center of the open field and horizontal movements were monitored for 15 min using a CCD camera. The images were processed using Image J OF software (O'Hara, Tokyo, Japan). Total activity for 15 min was used in statistical analysis.

Elevated plus maze test

Three-month-old male mice were used. An elevated plus maze [closed arms: 25 × 5 × 15

cm (H); open arms 25 × 5 × 0.3 cm (H)] was used in a soundproof room [2 m × 2 m × 2 m (H)]. The floor of each arm was made of white plastic and the walls and ridges were made of clear plastic. Closed arms and open arms were orthogonally arranged, 60 cm above the floor. The light level was 70 lux at the center of the maze platform (5 × 5 cm). Individual mice were put onto the center platform facing an open arm and mice were allowed to move freely in the maze for 5 min. Total distance traveled, % time in the open arms and % of entries to the open arms were measured as indices. Data were collected and analyzed using Image J EPM software (O'Hara, Tokyo, Japan).

Novelty suppressed feeding test

Four-month-old male mice were weighed and food was removed from the cage. However, water was available *ad libitum*. Twenty-four hours after food restriction, mice were transferred to a testing room and placed in a novel arena with a Petri dish containing a food pellet in the center. Each subject was placed in the corner of the testing area, and the latency to eat the pellet was recorded during a 10 min-period. All experiments were performed using normal, ambient, overhead lighting and were performed during the light phase of the cycle, between 13:00 and 18:00 h.

Eight-arm radial maze test

All training and testing was performed with 4-month-old male mice in an open, white, one-unit, eight-arm radial maze with 11.5 cm high transparent walls and
9.0 cm wide corridors. The eight arms radiated equidistantly from a circular central area, with a diameter of 29.0 cm. Each arm was 40.5 cm long, and at the end of the arm, a circular food well (diameter: 1.5 cm, depth: 0.5 cm) contained 25 mg food pellets (Precision Food Pellets, O'Hara, Tokyo, Japan). The maze was placed in the middle of a well-lit room and no other animals were present during training and testing. A multitude of two- and three-dimensional distal cues were available. During the training trials, four arms were baited. The same arms remained baited for all training and retention trials. Four patterns of baited arms were used, and the patterns were chosen to reflect equal difficulty and minimize non-spatial search strategies (*i.e.*, > two consecutive visits to un-baited arms).

Four massed trials were conducted per day for each subject, which was preceded by a

1-min confinement in the center platform. The trial was terminated when the mouse entered and ate from all baited arms, or following a maximum latency of 10 min. At the end of 10 trials, the mouse was returned to the home cage. This procedure was repeated for nine training days (36 trials in total). Retention testing was conducted 24 h after the final training trials, with four trials as described under the training procedure. Horizontal movements and arm entries were monitored for 10 min using a CCD camera. Images were processed using Image J OF software (O'Hara, Tokyo, Japan) and animals were scored based on number of entries into baited and un-baited arms, time to retrieve bait rewards, and sequence of arms visited. The number of arm entries/minute was also recorded. Data were analyzed for the following measures: % correct, number of reference memory errors, and number of working memory errors. Reference memory errors were scored when the mouse visited an arm that was never baited with food. Working memory errors were scored when a mouse revisited an arm during a trial from which it obtained the food reward.

Y-maze test

Three-month-old male mice were used. The Y-maze apparatus (O'Hara, Tokyo, Japan) was made of gray plastic and consisted of three compartments [3 cm (W) bottom and 10 cm (W) top, 40 cm (L) and 12 cm (H)] radiating out from a center platform (a 3 × 3 × 3 cm triangle). The maze was set 80 cm above the floor, and desks and test apparatus surrounding the maze provided spatial cues. Each mouse was placed in the center of the maze facing one of the arms and was allowed to freely explore for 5 min. Experiments were performed at a light intensity of 70 lux (center of platform). An arm entry was defined as four legs entering one of the arms, and the sequence of entries was quantified using a TV monitor, which was behind a partition. An alternation was defined as consecutive entry into all three arms (the maximum number of alternations was the total number of entries minus 2). Percent alternation was calculated as (actual alternations/maximum alternations)/100. Percent alternation was designated as spontaneous alternation behavior and represented working memory.

Zero maze test

A zero maze (O'Hara, Tokyo, Japan; 40 cm diameter, 5 cm width), which consisted of two enclosed areas and two open areas, was used in a soundproof room (2 m × 2 m × 2 m (H)

and 50 cm above the floor), and 5-month-old male mice were used. Mice were placed in the closed section of the maze and were allowed free access to all maze areas for 5 min (luminescence: 70 lux). Total distance travelled, % time in open arms, and % of entries into open arms were measured as indices. Data were collected and analyzed using Image J OF software (O'Hara, Tokyo, Japan).

Morris water maze

A circular maze made of white plastic (1 m diameter, 30 cm depth) was filled with water to approximately 20 cm in depth (about 25°C), and 4-month-old male mice were used for testing. The water was colored with white paint so that the mice could not see the platform (20 cm high, 10 cm diameter; 1 cm below the water surface) or other cues under the water. Extra-maze landmark cues (*i.e.*, calendar, figure, plastic box) were visible to the mice. Mouse movements were recorded in the maze and analyzed using Image J WM (O'Hara, Tokyo, Japan). The mice underwent six trials (one session) per day for 4 consecutive days. Each acquisition trial was initiated by randomly placing the mouse into the water facing the outer maze edge at one of four designated starting points. However, the position of the submerged platform remained constant for each mouse throughout testing. A trial was terminated when the mouse reached the platform, and latency and distance swam were measured. Cut-off time of the trial was 60 s, and mice that did not reach the platform within 60 s were removed from the water and placed on the platform for 30 s before being dried and placed back into the home cage. The inter-trial interval was approximately 6 min. After 4 days of training, a probe test was conducted. During the probe test, the platform was removed. Each mouse was placed into the water at the point opposite the target platform and was allowed to swim in the maze for 60 s. Distance swum, number of target quadrant crossings and remaining three quadrants crossings, and time spent in each quadrant were measured.

Barnes maze

On the first day, habituation training was conducted with 3-month-old male mice. Individual mice were placed on the center of the maze, which consists of a circular table with 12 circular holes around the circumference of the table, and allowed to freely explore (5 min/mouse, without escape cage). Following habituation training, escape trainings were

conducted. For escape training, mice were placed into a small, plastic container in the maze center for 10 sec. The container was then opened and mice were led to the escape hole, and then allowed to escape into the hole (the tail was gently pinched if necessary). Escape training was repeated five times by altering the escape hole position (*e.g.*, 1, 3, 5, 8 and 11). Escape trainings were conducted for four days (three times/day). Each trial was terminated when the mouse escaped into the correct hole (cage), within a maximum of 120 sec after the start. Mice were left in the cage for 30 sec and then returned to the home cage. The inter-trial interval was approximately 15 min. Following the final escape training on the fifth day, probe tests were performed for a duration of 120 sec using the same paradigm as for maze training, except for the absence of a target cage.

Contextual fear Conditioning

Fear conditioning was performed with 3-month-old male mice and consisted of three parts: conditioning trial (Day 1), context test trial (Day 2), and cued test trial (Day 3). Mice were placed in a clear plastic chamber equipped with a stainless steel grid floor (34 × 26 × 30 (H) cm), which was wired to a shock generator. Mouse behavior was monitored and recorded using a CCD camera equipped to the chamber ceiling. White noise (65 dB) was supplied from a loudspeaker as an auditory cue (conditioned stimulus, CS). An unconditioned stimulus (US) (foot-shock: 0.5 mA, 2 sec) was administered at the end of the 30-sec CS period. The conditioning trial consisted of a 2-min exploration period, followed by two CS-US pairings, separated by 1 min each. 24 h after conditioning trials, context tests were performed in the same conditioning chamber for 3 min in the absence of white noise. Furthermore, a cued test was performed in an alternative context with distinct cues; the test chamber varied from the conditioning chamber in brightness (by 0-1 lux), color (white), floor structure (no grid) and shape (triangular). The cued test was conducted 24 h after the contextual test was finished; it consisted of a 2-min exploration period (no CS) to evaluate nonspecific contextual fear, followed by a 2-min CS period (no foot shock) to evaluate acquired cued fear. Rate of freezing response (immobility, excluding respiration and heartbeat) was measured as an index of fear memory. Data were collected and analyzed using Image J FZ2 software (O'Hara, Tokyo, Japan).

Forced swim test

Four-month-old male mice were placed into plastic buckets (19 cm in diameter and 23 cm deep), which contained 25°C water. Mobility was recorded for 6 min. The last 5 min were scored for immobility. Immobility duration was scored and analyzed using FST software (O'Hara, Tokyo, Japan).

Tail suspension test

Three-month-old male mice were held by the tail using adhesive tape placed approximately 1.5 cm from the tip of the tail, which was attached to a wire 30 cm above the floor. Movement was monitored for 5 min using a CCD camera, and immobility duration was scored and analyzed using Image J TS software (O'Hara, Tokyo, Japan).

Sucrose preference test

Five-month-old male mice were used to determine preference for sucrose solution, as previously described (6). Mice were placed in their home cages and provided with access to two water bottles, one with water and the other with a 2% sucrose solution. The amount of each liquid consumed over a 48-h period was measured.

Theta oscillation recording

A commercial miniature electrode interface printed circuit board (PCB) with an Omnetics connector (EIB-27 micro, Neuralynx, AZ, USA) was used to construct an implantable electrode array. Two square, metallic rods (~1 mm across) were soldered to the PCB, which held a cannula (~0.2 mm diameter). Four insulated tungsten microwires (California Fine Wire), which served as recording electrodes, were inserted through the cannula and were connected to the PCB using gold connecting pins (EIB Pins Small, Neuralynx). Electrode tips were cut with fine scissors, and electrode lengths were adjusted so that the tips were ~200-300 μm apart. Male, CAPS2 KO and WT littermates, aged 8 and 12 weeks, were used in the chronic recording study. The mice were anesthetized with a cocktail solution containing 2% ketamine and 0.1% xylazine (10 ml/kg). Two small, 1-mm diameter holes were drilled above the cerebellar cortex, and a screw electrode was placed in each hole, which served as ground and reference for differential recording. A small craniotomy was made on the right side of the skull at 1.7 mm posterior to bregma and 1.0 mm lateral from the midline. The electrode array was inserted through the dura mater and the longest

electrode reached a depth of 2.0 mm from the surface. The craniotomy was then covered with a mixture of paraffin and paraffin oil, and the headstage was rigidly cemented with dental acrylic (Super-Bond C&B, Sun Medical, Shiga, Japan). After the dental acrylic was solidified, a protective wall of one-sided vinyl laminated paper was attached around the headstage. Chronic electrophysiological recordings were performed five days after surgery. Once the preamplifier cable was plugged into the headstage, at least 30 min of settling time was allowed prior to recording. Sleep recordings were performed in home cages. While the animal was sleeping, REM sleep was recognized by the appearance of theta (6-12 Hz) activity, which was preceded by a slow-wave sleep EEG pattern. At the end of REM sleep, theta activity disappeared. Occasionally, the mouse exhibited a brief twitch-like motion, followed by resumed sleep. During some recordings, mice behavior was simultaneously videotaped. Electrophysiological data were obtained from four electrodes and were simultaneously digitized at 32.556 kHz (bandwidth 0.1 Hz to 9 kHz) using a 16-bit multi-channel data acquisition system (Digital Lynx, Neuralynx). For analysis of EEG, acquired data were digitally re-sampled to 1.25 kHz and analyzed using custom software written with MATLAB (7).

4. References

1. Sadakata T, et al. (2007) Autistic-like phenotypes in Cadps2-knockout mice and aberrant CADPS2 splicing in autistic patients. J Clin Invest
2. 117:931-943.
3. Tamamaki N, et al. (2003) Green fluorescent protein expression and colocalization with calretinin, parvalbumin, and somatostatin in the GAD67-GFP knock-in mouse. J Comp Neurol 467:60-79.
4. Sadakata T, Mizoguchi A, Sato Y, Katoh-Semba R, Fukuda M, Mikoshiba K, Furuichi T (2004) The secretory granule-associated protein CAPS2 regulates neurotrophin release and cell survival. J Neurosci 24(1):43-52.
5. Shiraishi Y, Mizutani A, Yuasa S, Mikoshiba K, & Furuichi T (2004) Differential expression of Homer family proteins in the developing mouse brain. J Comp Neurol 473:582-599.
6. Liu L, et al. (2004) Role of NMDA receptor subtypes in governing the direction of hippocampal synaptic plasticity. Science 304(5673):1021-1024.
7. Maguire J & Mody I (2008) GABA(A)R plasticity during pregnancy: relevance to postpartum depression. Neuron 59(2):207-213.
8. Sakatani S, Seto-Ohshima A, Itohara S, & Hirase H (2007) Impact of S100B on local field potential patterns in anesthetized and kainic acid-induced seizure conditions in vivo. Eur J Neurosci 25(4):1144-1154.

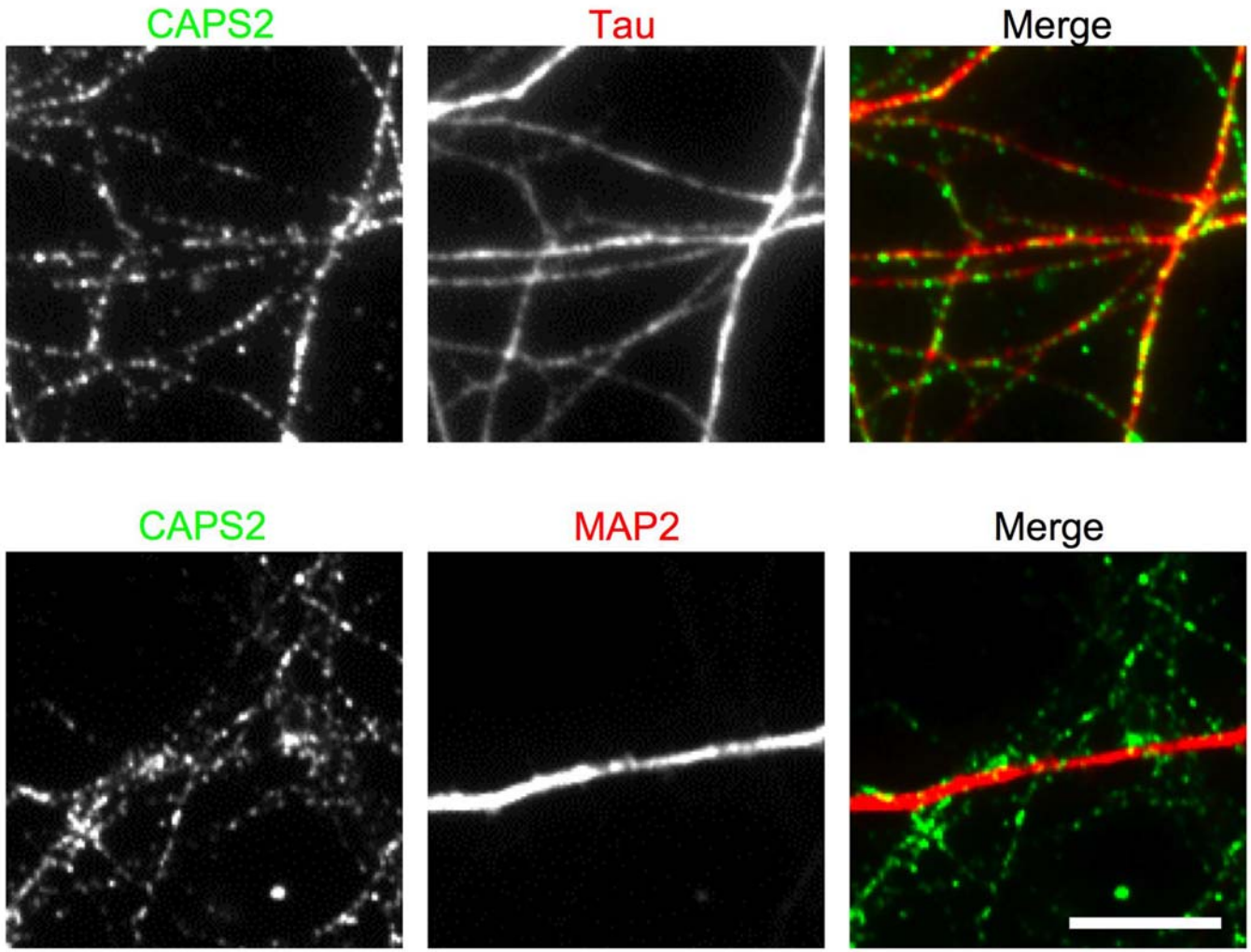
CAPS2
Tau
Merge
CAPS2
MAP2
Merge

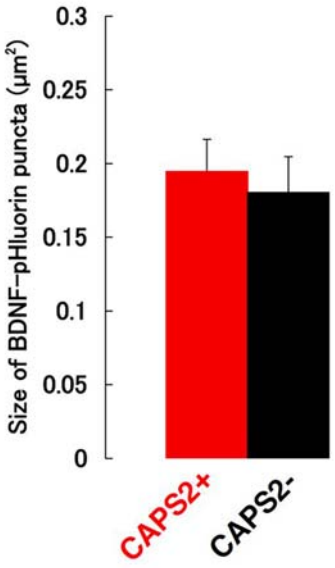
0.3
0.25
0.2
0.15
0.1
0.05
0
Size of BDNF-pHluorin puncta (μm²)
CAPS2+
CAPS2-

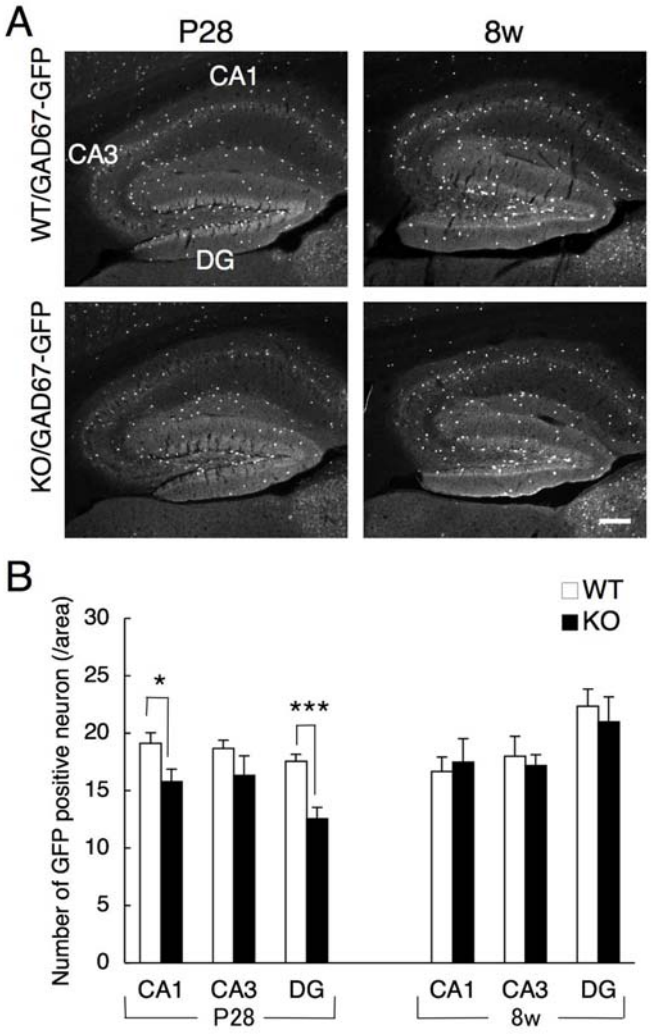
A
P28
8w
CA1
CA3
DG
WT/GAD67-GFP
KO/GAD67-GFP
B
WT
KO
Number of GFP positive neuron (/area)
30
25
20
15
10
5
0
*
***
CA1
CA3
DG
P28
CA1
CA3
DG
8w

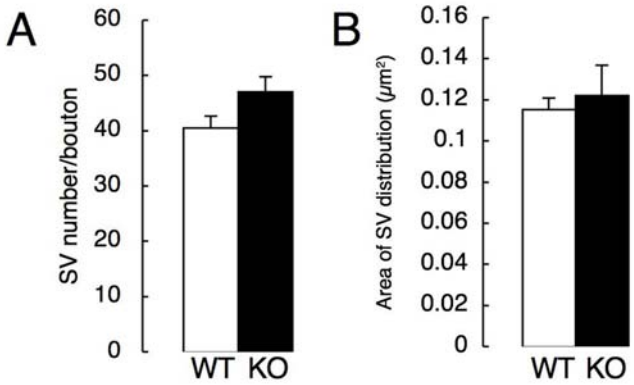
A
SV number/bouton
60
50
40
30
20
10
0
WT
KO
B
Area of SV distribution (μm²)
0.16
0.14
0.12
0.1
0.08
0.06
0.04
0.02
0
WT
KO

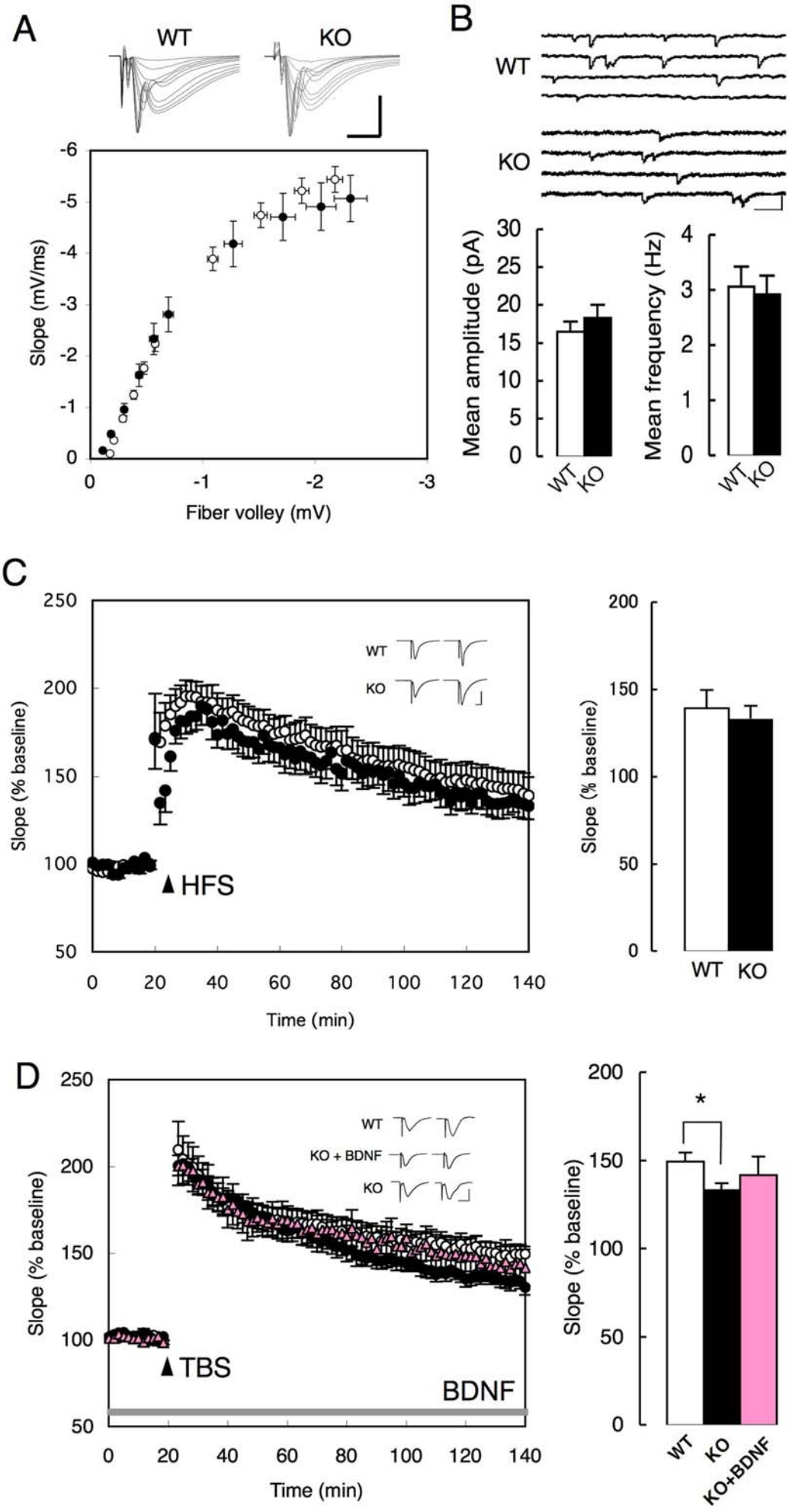
A
WT
KO
Slope (mV/ms)
Fiber volley (mV)
B
WT
KO
Mean amplitude (pA)
Mean frequency (Hz)
C
WT
KO
HFS
Slope (% baseline)
Time (min)
D
WT
KO + BDNF
KO
TBS
BDNF
Slope (% baseline)
Time (min)
*
WT
KO
KO+BDNF

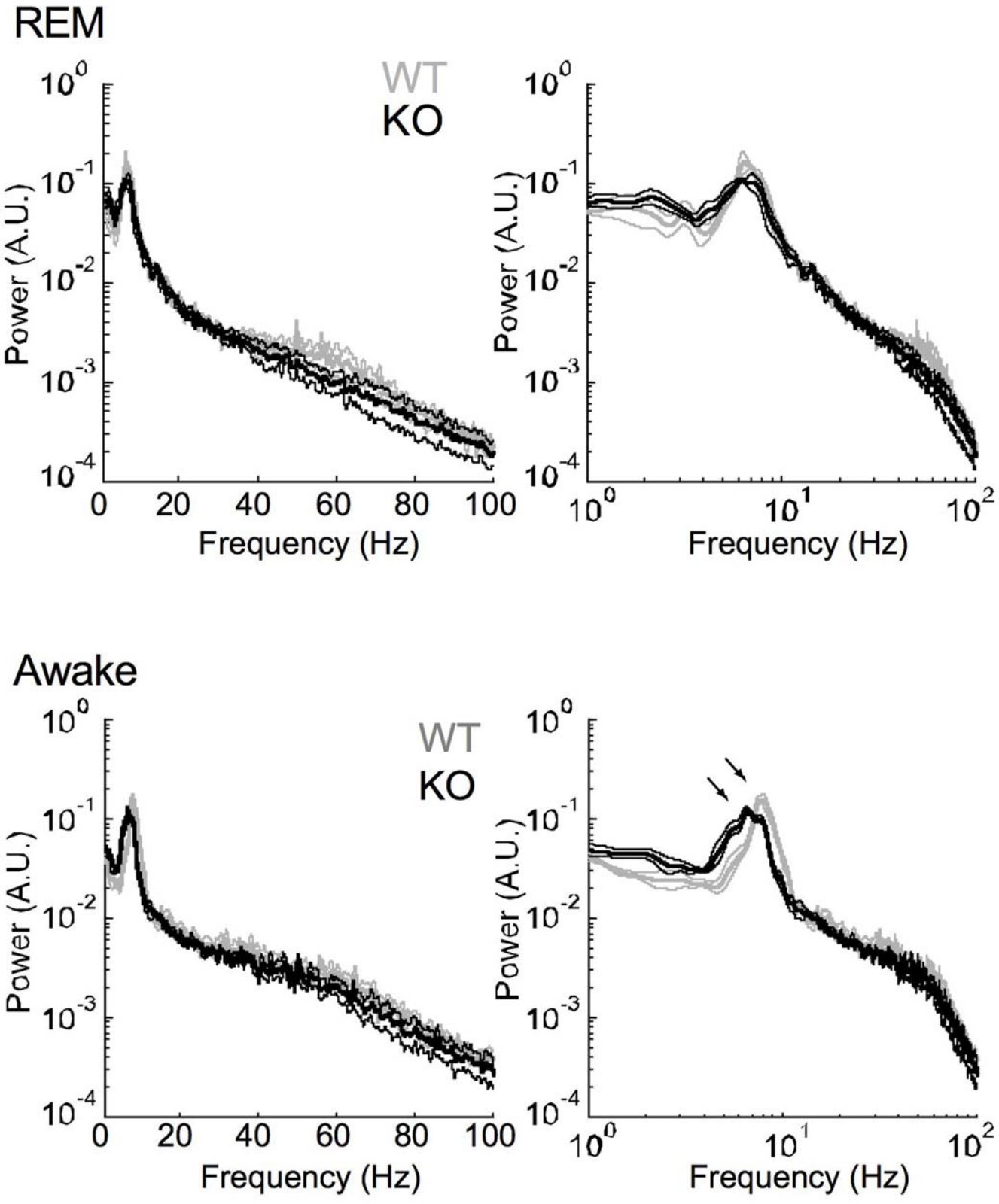
REM
WT
KO
Power (A.U.)
Frequency (Hz)
Awake
WT
KO
Power (A.U.)
Frequency (Hz)

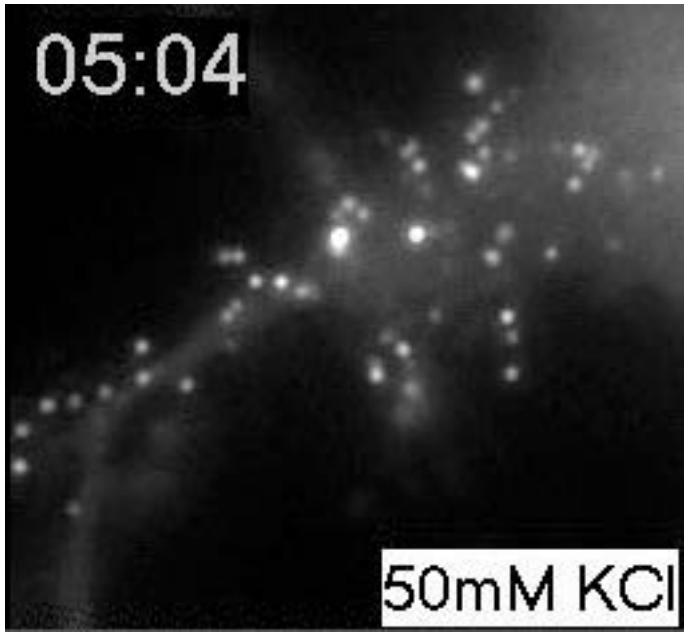
05:04
50mM KCl

Table S1 CAPS2 KO mice exhibit increased anxiety-like behavior

Anxiety	WT	KO	*P*
Open field (% time in center)	17.7±0.9	16.1±2.1	ns
Open field (total distance: AU)	5200±325	4892±504	ns
Open field - novel object (% time in center)	17.2±1.4	3.8±2.9	**
Open field - novel object (total distance: AU)	6840±482	4518±1024	*
Elevated plus maze (% time in open arm)	20.9±4.9	3.2±1.7	*
Novelty suppressed feeding (latency: sec)	114±29	217±36	*
8-arm radial maze (number of total arm choices)	10.8±0.3	7.8±0.2	***
Y-maze (number of total arm choices)	20.2±1.3	15.7±1.1	*
Zero maze (% time in open arm)	45.4±1.1	45.5±1.2	ns
Learning and memory	WT	KO	*P*
8-arm radial maze (reference memory error: %)	42.6±1.2	47.6±1.8	*
8-arm radial maze (working memory error: %)	36.0±1.5	34.1±0.7	ns
Morris water maze (% in quadrant)	22.3±4.4	22.1±7.1	ns
Y-maze (% alteration)	63.9±3.4	62.8±3.9	ns
Barnes maze (% target)	45.1±4.2	55.8±4.9	ns
Contextual fear (% freezing)	16.5±2.9	20.1±3.5	ns
Depression	WT	KO	*P*
Forced swim (time immobile: sec)	118.3±9.3	145.7±8.4	*
Tail suspension (time immobile: sec)	75.0±6.5	70.4±6.0	ns
Sucrose preference (% sucrose)	85.0±0.8	83.5±1.8	ns

AU: arbitrary unit. ns: not significant. *P<0.05, **P<0.01, and ***P<0.001 using the Student's t-test.